



Reflection and transmission at low concentration by a depth-varying random distribution of cylinders in a fluid slab-like region

J.M. Conoir^{a,*}, S. Robert^b, A. El Mouhtadi^c, F. Luppé^c

^aUPMC Univ Paris 06, UMR 7190, Institut Jean Le Rond d'Alembert, F-75005 Paris, France

^bLaboratoire Ondes et Acoustique, UMR CNRS 7587, ESPCI, 10 rue Vauquelin, 75231 Paris Cedex 05, France

^cLaboratoire Ondes et Milieux Complexes, FRE CNRS 3102, Groupe Ondes Acoustiques, Université du Havre, Place R. Schuman, 76610 Le Havre, France

ARTICLE INFO

Article history:

Received 7 November 2008

Received in revised form 11 June 2009

Accepted 17 June 2009

Available online 21 June 2009

Keywords:

Multiple scattering

Coherent waves

Effective mass density

Boundary conditions

Reflection and transmission

ABSTRACT

This paper deals with multiple scattering by a random arrangement of parallel circular elastic cylinders immersed in a fluid. The cylinders are distributed in a region called “slab” that is located between two parallel planes orthogonal to a given x -direction. The disorder inside the slab depends on the x -variable. The goal is to calculate the reflection and transmission coefficients by this space-varying slab. For low concentrations of cylinders, two methods are developed from Twersky's theory on the propagation of coherent waves in an effective medium. The first method is based upon the discretization of the properties of the space-varying slab. The second one is based on the WKB method. They are successfully compared in the case of a smooth space-varying slab in which the random distribution of cylinders varies slowly along the x -direction. An effective mass density is defined, which allows the derivation of the mean acoustic displacement from the mean pressure field. The continuity of both pressure and normal displacement is thus shown at the interface between two different effective media as well as at the interface between the space-varying slab and a homogeneous fluid.

© 2009 Elsevier B.V. All rights reserved.

1. Introduction

Multiple scattering by random arrangements of scatterers is a topic with an extensive literature. See, for example, the recent books by Tsang et al. [1] and Martin [2]. A typical problem is the following. The space is filled with a homogeneous compressible fluid of density ρ and sound speed c , and a fluid slab-like region, $0 \leq x \leq d$, contains many randomly spaced scatterers. In the following, the scatterers are elastic parallel circular cylinders, with axes normal to the x direction, so that the problem is a two-dimensional one (cf. Fig. 1). As a time harmonic plane wave with wavenumber $k = \omega/c$ (ω is the angular frequency) is incident upon the slab (cf. Fig. 1), what are the reflected and transmitted waves? The acoustic fields cannot be computed exactly for a large number of cylinders. This is the reason why another problem is solved. The slab is replaced by a homogeneous effective medium in which coherent plane waves propagate. After Twersky [3], coherent plane waves can be interpreted as the average of the exact fields calculated for a great number of random configurations of the scatterers. They are characterized by a complex wavenumber K_{eff} usually called *effective wavenumber*. The earliest modern work on such a problem is due to Foldy [4] and a large number of papers have been published since. Most of them are mainly focused on the effective wavenumber calculation [5–15], while few of them actually deal with the reflected and transmitted fields

* Corresponding author. Tel.: +33 1 44 27 49 28; fax: +33 1 44 27 52 68.

E-mail address: conoir@lmm.jussieu.fr (J.M. Conoir).

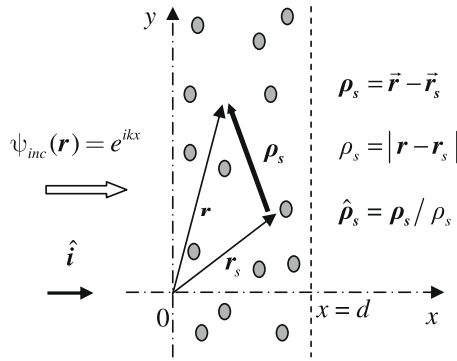


Fig. 1. Geometry of the uniform slab.

[16–21]. This point is important to notice because it is not obvious to relate the reflection and transmission coefficients of the slab, R_{slab} and T_{slab} , to the effective wavenumber. Nonetheless, it has been shown in Refs. [16,19,21,22] that

$$R_{slab} = R_{12} + \frac{T_{12}e^{iK_{eff}d}R_{21}e^{iK_{eff}d}T_{21}}{1 - R_{21}^2e^{2iK_{eff}d}} = R_{12} + T_{12}e^{iK_{eff}d}R_{21}e^{iK_{eff}d}T_{21} + \dots \tag{1.1}$$

$$T_{slab} = \frac{T_{12}e^{iK_{eff}d}T_{21}}{1 - R_{21}^2e^{2iK_{eff}d}} = T_{12}e^{iK_{eff}d}T_{21} + T_{12}e^{iK_{eff}d}R_{21}^2e^{2iK_{eff}d}T_{21} + \dots \tag{1.2}$$

where R_{12} is the specular reflection coefficient at the first interface of the slab, T_{12} (T_{21}) is the transmission coefficient at the interface between the homogeneous fluid, labeled 1, (slab, labeled 2) and the slab, labeled 2, (homogeneous fluid, labeled 1), and R_{21} the specular reflection coefficient inside the slab (cf. Fig. 2). Eqs. (1.1) and (1.2) correspond to Eq. (21) in Ref. [16] and to Eqs. (42) and (46) in Ref. [19], with $-R_{12} = R_{21} = Q = Q'$ and $T_{12}T_{21} = 1 - Q^2$. Of course, the analytic expression of Q depends on the theory used: Q is defined in Ref. [16] for Twersky's theory (cf. Eq. (3.11)) and in Ref. [19] for Fikioris and Waterman's one (cf. Eq. (4.12)). The physical meaning of Eqs. (1.1) and (1.2) is clear. First, the slab looks like a fluid plate in which waves propagate with wavenumber K_{eff} . Second, the slab can be considered as a usual Fabry–Perrot interferometer (cf. Fig. 2).

If the concentration of scatterers is low enough, the impedance ratio between the homogeneous fluid and the slab is close to 1, so that $|R_{21}| \approx 0$ and $|T_{12}| \approx |T_{21}| \approx 1$. It follows that T_{slab} can be approximated by

$$T_{slab} \approx e^{iK_{eff}d} \tag{1.3}$$

so that

$$\text{Im}(K_{eff}) \approx -\text{Log}|T_{slab}|/d \tag{1.4}$$

This last relation has indeed been successfully used, at low concentration, in order to evaluate the attenuation of the coherent waves that propagate through the slab from experimental transmission data [23,24].

In all the papers cited previously and even for scatterers of different size [25], the random distribution of scatterers is always assumed to be uniform in space. However, in many cases, as in sediment suspensions, bubbles, colloids, the concentration of scatterers depends on space. It is also the case for polydisperse media when a significant number of smaller par-

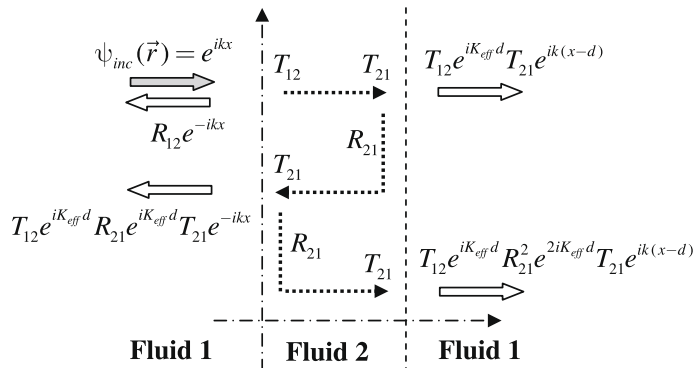


Fig. 2. Reflection and transmission by the uniform slab.

ticles can fit into the interstices between the larger ones. Clustering, or non-uniform concentration of particles, is commonly found to occur as a result of scatterers entrainment in fluid flows. In such cases, the *particle size distribution* can be strongly modified and the propagation of waves as well [26]. Our paper deals with a similar but simpler case, the reflected and transmitted waves by a slab in which the concentration and/or the size of the scatterers, rather than uniform, depends on the x -space variable. The goal is the generalization of Eqs. (1.1) and (1.2) to such a space-varying slab. Two different methods are developed. In the first one, the space-varying slab is discretized into several layers in which the random distribution of scatterers is uniform and an effective medium theory is developed in each. In other words, the space-varying slab is considered as a stack of “uniform slabs”. In the second one, the spatial variations of the random distribution are assumed smooth enough for the relevancy of the WKB method [27]. For both methods, a crucial point is the knowledge of the boundary conditions at the interface between a homogeneous fluid and a uniform slab, as well as that at the interface between two different uniform slabs. The continuity of pressure between the surrounding homogeneous fluid and a uniform slab has been shown in Refs. [16,19], as used in the derivation of Eqs. (1.1) and (1.2). Surprisingly enough, however, continuity of the normal displacement is not required in this derivation. We still do not understand clearly the reason why it is not needed in the calculation of the reflection and transmission coefficients of Eqs. (1.1) and (1.2), but we show nonetheless that this latter continuity condition is fulfilled at all interfaces, as well as that on pressure. This is achieved after defining an effective mass density ρ_{eff} for the uniform slab, as in [28], that allows the derivation of the displacement expression from that of pressure.

The important point worth to notice is that the problem of an acoustic field incident upon the random medium, whatever its geometry, is equivalent to that of the same acoustic field incident upon a homogeneous dissipative fluid medium, only if the usual continuity conditions at the interfaces of the equivalent medium apply. If so, the more practical problem of scatterers in a cylindrical medium, for example, turns to the rather well known problem of scattering by a cylinder of density ρ_{eff} and complex wavenumber K_{eff} at a given angular frequency ω [29].

In order to be more explicit, it should be underlined that demonstration of the continuity of normal displacement requires an analytical expression of the effective mass density. This is the main reason why Twersky’s theory is used here. Of course, it should be better to deal with the Linton and Martin’s approach [15]. This one leads to a better approximation of the effective wavenumber, as compared to the Waterman and Truell’s expression of the effective wavenumbers that is found in Twersky’s theory [6]. But the analytic expression of the effective mass density in Linton and Martin’s approach is not known yet. Anyway, the Waterman and Truell’s effective wavenumber is close to that of Linton and Martin at low concentration [19]. So, the use of Twersky’s theory is justified here, as low concentrations of scatterers are considered. This is clearly a limitation of the method presented.

The effective mass density of a uniform slab is defined in Section 2, and the Foldy–Twersky’s integral equations that govern the average acoustic pressure fields are derived in Section 3. These are the common starting points of the two methods developed to calculate the reflection and transmission coefficients of the space-varying slab. Section 4 presents the method based on the discretization of the slab. The reflection and transmission coefficients are calculated after resolution of a linear set of equations of rank $2N$ with N the number of uniform layers. The boundary conditions at the interfaces of the slab are derived in Section 5 from the equations established in the preceding section. The effective mass density defined in Section 2 is used to link the pressure field to the displacement field, so that the boundary conditions on pressure and normal displacement are fulfilled even for the interfaces between two different uniform slabs. These boundary conditions are used in Section 6 to write the reflection and transmission coefficients found in Section 4 as Debye’s series, more suitable for the computations, which generalize Eqs. (1.1) and (1.2) to the discretized space-varying slab. Section 7 presents the method based on the WKB one, for a slab of smooth spatial variations. The knowledge of the boundary conditions at the interfaces of the slab with the surrounding fluid is essential in the method, because neither the theorem of extinction nor the Lorentz–Lorenz law can be used for space-varying slabs. Finally, Section 8 shows the numerical comparison of the different expressions found for the reflection and transmission coefficients.

2. Effective mass density of a uniform slab

In linear acoustics, Euler’s relation relates the time harmonic acoustic displacement \mathbf{u}_f in a fluid medium to the time harmonic pressure p ,

$$\mathbf{u}_f = \frac{1}{\rho_f \omega^2} \nabla p \quad (2.1)$$

with ρ_f the mass density of the fluid. This is the reason why the mass density is needed in order to write the continuity of normal displacement at the interface between two different fluids. While the mass density ρ_f of a homogeneous fluid is a known characteristic of the fluid, that of a uniform slab has yet to be defined. In order to do so, let us consider the R_{12} specular reflection coefficient at the interface between two fluids, labeled 1 and 2 respectively; its expression is given by Ref. [27], *i.e.*

$$R_{12} = \frac{\rho_2 k_1 - \rho_1 k_2}{\rho_2 k_1 + \rho_1 k_2} \quad (2.2)$$

with k_1 and k_2 the wavenumbers in fluids 1 and 2, and ρ_1 and ρ_2 the mass densities of the fluids. If fluid 2 contains a uniform distribution of scatterers, this specular reflection is obtained from Eq. (1.1) by letting the depth d of the slab tend to infinity: $R_{12} = \lim_{d \rightarrow +\infty} R_{slab} = -Q$ (the imaginary part of the effective wavenumber K_{eff} being positive). As k_2 is to be replaced with K_{eff} in Eq. (2.2) and ρ_2 with ρ_{eff} , it follows straightaway that

$$\rho_{eff} = \rho_1 \frac{K_{eff}}{k_1} \frac{1 - Q}{1 + Q} \tag{2.3}$$

Eq. (2.3) is the same as Eq. (2.1) of Ref. [28]. Consequently, the mass density of a homogeneous fluid with a uniform distribution of scatterers is complex and depends on frequency, as K_{eff} and Q do.

It should be pointed out that the continuity of normal displacement would be clearly verified if the displacement vector \mathbf{u}_f , averaged over all possible locations of the cylinders, was related to the averaged pressure $\langle p \rangle$ as $\langle \mathbf{u}_f \rangle = \nabla \langle p \rangle / \rho_f \omega^2$, but it is not the case. The mass density is an effective quantity that is affected by the average. In fact, it will be shown that the correct relation is

$$\langle \mathbf{u}_f \rangle = \nabla \langle p \rangle / \rho_{eff} \omega^2 \tag{2.4}$$

So, the knowledge of ρ_{eff} is needed to write the continuity of the normal displacement, which is done in Section 5, after Twersky's theory is developed in the following two sections.

3. Foldy–Twersky's integral equations

The two methods developed to calculate the reflection and transmission coefficients of a space-varying slab are based on a set of coupled integral equations that are derived, in this section, from Foldy–Twersky's integral equation. According to Ishimaru (cf. Ref. [30], Eqs. (14)–(34)), the $\langle \psi(\mathbf{r}) \rangle$ coherent pressure field inside the slab satisfies the Foldy–Twersky's integral equation

$$\langle \psi(\mathbf{r}) \rangle = \psi_{inc}(\mathbf{r}) + \int_{slab} T(\mathbf{r}, \mathbf{r}_s) \langle \psi(\mathbf{r}_s) \rangle n(\mathbf{r}_s) d\mathbf{r}_s \tag{3.1}$$

with $\psi_{inc}(\mathbf{r}) = \exp(ik_1x)$ the spatial dependence of the incident harmonic pressure wave, $n(\mathbf{r}_s) d\mathbf{r}_s$ the average number of scatterers in the $d\mathbf{r}_s$ small surface around \mathbf{r}_s , and $T(\mathbf{r}, \mathbf{r}_s) \langle \psi(\mathbf{r}_s) \rangle$ the field at \mathbf{r} due to the scatterer located at \mathbf{r}_s when $\langle \psi(\mathbf{r}_s) \rangle$ is incident (cf. Fig. 1). Under the far field hypothesis ($k_1 \rho_s = k_1 |\mathbf{r} - \mathbf{r}_s| \rightarrow +\infty$), the scattering operator $T(\mathbf{r}, \mathbf{r}_s)$ acting on $\langle \psi(\mathbf{r}_s) \rangle$ is defined as

$$T(\mathbf{r}, \mathbf{r}_s) \langle \psi(\mathbf{r}_s) \rangle = T(\hat{\mathbf{I}}, \hat{\rho}_s) \langle \psi(\mathbf{r}_s) \rangle G_0^\infty(\rho_s) = T(\hat{\mathbf{I}}, \hat{\rho}_s) \langle \psi(\mathbf{r}_s) \rangle \sqrt{\frac{2}{\pi}} \frac{e^{ik_1 \rho_s - i\frac{\pi}{4}}}{\sqrt{k_1 \rho_s}} \tag{3.2}$$

with $G_0^\infty(\rho_s)$ the far field expression of the two-dimensional Green's function $H_0^{(1)}(k_1 \rho_s)$. In Eq. (3.2), $T(\hat{\mathbf{I}}, \hat{\rho}_s) \langle \psi(\mathbf{r}_s) \rangle$ is the amplitude of the wave scattered by a single scatterer located at \mathbf{r}_s , in direction $\hat{\rho}_s = \rho_s / \rho_s$ with $\rho_s = \mathbf{r} - \mathbf{r}_s$ and $\rho_s = |\mathbf{r} - \mathbf{r}_s|$, of a plane incident wave of amplitude $\langle \psi(\mathbf{r}_s) \rangle$ propagating in any direction $\hat{\mathbf{I}}$. It does not depend on \mathbf{r} . As the incident wave and the geometry of the varying slab are supposed to be independent of the y -coordinate ($n(\mathbf{r}_s) = n(x_s)$), the same holds for the coherent field $\langle \psi(\mathbf{r}) \rangle$, $\langle \psi(\mathbf{r}) \rangle = \langle \psi(x) \rangle$, and the Foldy–Twersky's integral equation becomes

$$\langle \psi(x) \rangle = e^{ik_1 x} + \sqrt{\frac{2}{\pi}} e^{-i\frac{\pi}{4}} \int_0^d n(x_s) \left[\int_{-\infty}^{+\infty} T(\hat{\mathbf{I}}, \hat{\rho}_s) \langle \psi(x_s) \rangle \frac{e^{ik_1 \rho_s}}{\sqrt{k_1 \rho_s}} dy_s \right] dx_s \tag{3.3}$$

The integration with respect to y_s is performed with use of the stationary phase method assuming that $k_1 d$ is large enough. The stationary phase method is based on the very well known formula [31]

$$\int_{-\infty}^{+\infty} A(y_s) e^{ik_1 d S(y_s)} dy_s \underset{k_1 d \rightarrow +\infty}{=} \sqrt{\frac{2\pi}{k_1 d |S''(y_{sp})|}} A(y_{sp}) e^{ik_1 d S(y_{sp})} e^{i\frac{\pi}{4} \text{sgn}(S''(y_{sp}))} \tag{3.4}$$

with $\text{sgn}(\tilde{y}) = \pm 1$ ($\tilde{y} > 0$ or $\tilde{y} < 0$) and y_{sp} the saddle point, root of the saddle point equation $S'(y_s) = 0$, where a prime denotes a first order derivative and a double prime a second order derivative. In our case

$$S(y_s) = \rho_s / d = \sqrt{(x - x_s)^2 + (y - y_s)^2} / d \tag{3.5}$$

and the saddle point equation gives $y_s - y = 0$, so that its root is $y_{sp} = y$. It comes then, $S(y_{sp}) = |x - x_s| / d$, $S''(y_{sp}) = [S''(y_s)]_{y_s=y_{sp}} = 1/|x - x_s| d > 0$ and

$$\hat{\rho}_s(y_{sp}) = \left(\frac{x - x_s}{|x - x_s|}, 0 \right) = \pm \hat{\mathbf{i}} \quad (x > x_s \text{ or } x_s < x) \tag{3.6}$$

with $\hat{\mathbf{i}}$ defined in Fig. 1. It follows that (cf. Ref. [30], Eqs. (14–38))

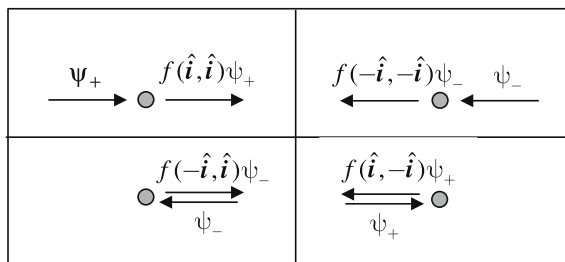


Fig. 3. Forward and backward scattering amplitudes.

$$\langle \psi(x) \rangle = e^{ik_1x} + \frac{2e^{ik_1x}}{k_1} \int_0^x T(\hat{\mathbf{i}}, \hat{\mathbf{i}}) \langle \psi(x_s) \rangle e^{-ik_1x_s} n(x_s) dx_s + \frac{2e^{-ik_1x}}{k_1} \int_x^d T(\hat{\mathbf{i}}, -\hat{\mathbf{i}}) \langle \psi(x_s) \rangle e^{ik_1x_s} n(x_s) dx_s \tag{3.7}$$

Following Twersky [16], $\langle \psi \rangle$ is decomposed into two fields, ψ_+ and ψ_- ,

$$\langle \psi \rangle = \psi_+ + \psi_-, \tag{3.8a}$$

with

$$\psi_+(x) = e^{ik_1x} + \frac{2}{k_1} \int_0^x T(\hat{\mathbf{i}}, \hat{\mathbf{i}}) \langle \psi(x_s) \rangle e^{ik_1(x-x_s)} n(x_s) dx_s \tag{3.8b}$$

$$\psi_-(x) = \frac{2}{k_1} \int_x^d T(\hat{\mathbf{i}}, -\hat{\mathbf{i}}) \langle \psi(x_s) \rangle e^{ik_1(x_s-x)} n(x_s) dx_s \tag{3.8c}$$

The integral in Eq. (3.8b) gives all the waves scattered from cylinders on the left-hand side of the observation point, while that in Eq. (3.8c) corresponds to the waves scattered from the cylinders on its right hand side. The scattered waves in both fields ψ_+ and ψ_- are due to the incidence of the mean total field $\langle \psi \rangle$, and propagate as homogeneous waves, with wavenumber k_1 , in the scattering medium; ψ_+ is composed of waves propagating from the left to the right, while the contrary stands for ψ_- . As a result, the propagation direction $\hat{\mathbf{i}}$ of any incident wave on a given scatterer is either $\hat{\mathbf{i}}$ or $-\hat{\mathbf{i}}$. Hence, Twersky defines $T(\hat{\mathbf{i}}, \pm\hat{\mathbf{i}}) \langle \psi(x_s) \rangle$ as follows:

$$T(\hat{\mathbf{i}}, \pm\hat{\mathbf{i}}) \langle \psi(x_s) \rangle = f(\hat{\mathbf{i}}, \pm\hat{\mathbf{i}}; x_s) \psi_+(x_s) + f(-\hat{\mathbf{i}}, \pm\hat{\mathbf{i}}; x_s) \psi_-(x_s) \tag{3.9}$$

In Eq. (3.9), as depicted in Fig. 3, $f(\pm\hat{\mathbf{i}}, \pm\hat{\mathbf{i}}; x_s)$ are the forward and backward scattering amplitudes associated to the scattering of a plane wave by a cylinder located at r_s . They can be expressed as modal sums, cf. [29,32], and calculated numerically. For circular cylinders, $f(-\hat{\mathbf{i}}, -\hat{\mathbf{i}}; x_s) = f(\hat{\mathbf{i}}, \hat{\mathbf{i}}; x_s)$ and $f(-\hat{\mathbf{i}}, \hat{\mathbf{i}}; x_s) = f(\hat{\mathbf{i}}, -\hat{\mathbf{i}}; x_s)$. The following set of coupled integral equations is then obtained by inserting Eqs. (3.8 and 3.9) into Eq. (3.7),

$$\psi_+(x) = e^{ik_1x} + \int_0^x [T(x_s)\psi_+(x_s) + R(x_s)\psi_-(x_s)] e^{ik_1(x-x_s)} n(x_s) dx_s \tag{3.10a}$$

$$\psi_-(x) = \int_x^d [R(x_s)\psi_+(x_s) + T(x_s)\psi_-(x_s)] e^{+ik_1(x_s-x)} n(x_s) dx_s \tag{3.10b}$$

with

$$T(x_s) = \frac{2}{k_1} f(\hat{\mathbf{i}}, \hat{\mathbf{i}}; x_s) \quad \text{and} \quad R(x_s) = \frac{2}{k_1} f(\hat{\mathbf{i}}, -\hat{\mathbf{i}}; x_s). \tag{3.11}$$

Eq. (3.10) are the starting point of the two methods developed in the following sections to calculate the reflection and transmission coefficients of the space-varying slab.

4. Discretization of the space-varying slab

In this section, the space-varying slab is discretized into N layers in which the random distribution of scatterers is uniform (cf. Fig. 4). For each layer number j ($1 \leq j \leq N$), $n(x_j) = n_j$ is the number of scatterers per unit surface, and all scatterers are identical and characterized by

$$T^{(j)} = T(x_j)n(x_j) = \frac{2n_j}{k_1} f_j(\hat{\mathbf{i}}, \hat{\mathbf{i}}) \quad \text{and} \quad R^{(j)} = R(x_j)n(x_j) = \frac{2n_j}{k_1} f_j(\hat{\mathbf{i}}, -\hat{\mathbf{i}}) \tag{4.1}$$

with $f_j(\hat{\mathbf{i}}, \pm\hat{\mathbf{i}})$ the forward and backward scattering amplitudes of the cylinders located in the j th uniform slab $x_{j-1} \leq x \leq x_j$ ($1 \leq j \leq N$). As previously, the $\langle \psi^{(j)} \rangle$ coherent field inside each uniform slab $x_{j-1} \leq x \leq x_j$ is decomposed as

$$\langle \psi^{(j)} \rangle = \psi_+^{(j)} + \psi_-^{(j)} \tag{4.2}$$

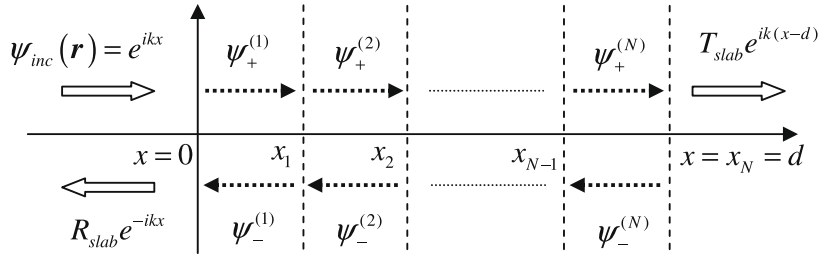


Fig. 4. The discretized slab.

In addition to what happens for a uniform single slab [16], the coupled integral equations Eq. (3.10) have now to be split into N coupled integral equations. It follows that for $0 \leq x \leq x_1$

$$\psi_+^{(1)}(x) = e^{ik_1x} + e^{ik_1x} \int_0^x [T^{(1)}\psi_+^{(1)}(x_s) + R^{(1)}\psi_-^{(1)}(x_s)] e^{-ik_1x_s} dx_s \tag{4.3a}$$

$$\begin{aligned} \psi_-^{(1)}(x) &= e^{-ik_1x} \int_x^{x_1} [R^{(1)}\psi_+^{(1)}(x_s) + T^{(1)}\psi_-^{(1)}(x_s)] e^{+ik_1x_s} dx_s \\ &+ e^{-ik_1x} \sum_{m=2}^N \int_{x_{m-1}}^{x_m} [R^{(m)}\psi_+^{(m)}(x_s) + T^{(m)}\psi_-^{(m)}(x_s)] e^{+ik_1x_s} dx_s \end{aligned} \tag{4.3b}$$

for $x_{j-1} \leq x \leq x_j (2 \leq j \leq N-1)$

$$\begin{aligned} \psi_+^{(j)}(x) &= e^{ik_1x} + e^{ik_1x} \sum_{m=1}^{j-1} \int_{x_{m-1}}^{x_m} [T^{(m)}\psi_+^{(m)}(x_s) + R^{(m)}\psi_-^{(m)}(x_s)] e^{-ik_1x_s} dx_s \\ &+ e^{ik_1x} \int_{x_{j-1}}^x [T^{(j)}\psi_+^{(j)}(x_s) + R^{(j)}\psi_-^{(j)}(x_s)] e^{-ik_1x_s} dx_s \end{aligned} \tag{4.4a}$$

$$\begin{aligned} \psi_-^{(j)}(x) &= e^{-ik_1x} \int_x^{x_j} [R^{(j)}\psi_+^{(j)}(x_s) + T^{(j)}\psi_-^{(j)}(x_s)] e^{+ik_1x_s} dx_s \\ &+ e^{-ik_1x} \sum_{m=j+1}^N \int_{x_{m-1}}^{x_m} [R^{(m)}\psi_+^{(m)}(x_s) + T^{(m)}\psi_-^{(m)}(x_s)] e^{+ik_1x_s} dx_s \end{aligned} \tag{4.4b}$$

for $x_{N-1} \leq x \leq x_N$

$$\begin{aligned} \psi_+^{(N)}(x) &= e^{+ik_1x} + e^{ik_1x} \sum_{m=1}^{N-1} \int_{x_{m-1}}^{x_m} [T^{(m)}\psi_+^{(m)}(x_s) + R^{(m)}\psi_-^{(m)}(x_s)] e^{-ik_1x_s} dx_s \\ &+ e^{ik_1x} \int_{x_{N-1}}^x [T^{(N)}\psi_+^{(N)}(x_s) + R^{(N)}\psi_-^{(N)}(x_s)] e^{-ik_1x_s} dx_s \end{aligned} \tag{4.5a}$$

$$\psi_-^{(N)}(x) = e^{-ik_1x} \int_x^{x_N} [R^{(N)}\psi_+^{(N)}(x_s) + T^{(N)}\psi_-^{(N)}(x_s)] e^{ik_1x_s} dx_s \tag{4.5b}$$

As it is assumed that coherent waves propagate in each uniform slab, the solutions of Eqs. (4.3–4.5) are searched for as follows

$$\psi_{\pm}^{(j)} = A_{\pm}^{(j)} e^{ik_{eff}^{(j)}x} + B_{\pm}^{(j)} e^{-ik_{eff}^{(j)}x} \tag{4.6}$$

with $K_{eff}^{(j)}$ the effective wavenumber associated to coherent waves propagating in the uniform slab $x_{j-1} \leq x \leq x_j (1 \leq j \leq N)$. Both $\psi_+^{(j)}$ and $\psi_-^{(j)}$ are thus composed of two coherent waves that propagate respectively in directions $+\hat{i}$ and $-\hat{i}$. At first sight, this seems to be inconsistent with the discussion given after Eq. (3.10), in which ψ_+ (resp. ψ_-) was said to be composed of homogeneous waves propagating in the $+\hat{i}$ direction (resp. $-\hat{i}$). This apparent inconsistency vanishes, however, when one remembers that a homogeneous wave scattered by a cylinder in the $\pm\hat{i}$ direction is due both to incident homogeneous waves that were propagating in the same direction and to waves that were propagating in the opposite direction. In other words, while Eq. (4.6) provide a global description in the effective medium, i.e. in the absence of scatterers, Eq. (3.10) gave a local description of the multiple scattering process in the original medium, i.e. that with scatterers. In short, $\psi_+^{(j)}$ and $\psi_-^{(j)}$, in Eq. (3.10), must not be interpreted each as a single plane wave that propagates in the $\pm\hat{i}$ direction, as in Eq. (4.6), but as acoustic fields due to a sum of plane waves that propagate in the $\pm\hat{i}$ direction. It follows from Eq. (4.6) that there are $4N$ unknown amplitudes ($A_{\pm}^{(j)}, B_{\pm}^{(j)}$) and N unknown effective wavenumbers $K_{eff}^{(j)}$. Once Eq. (4.6) are introduced into Eqs. (4.3–4.5), one gets for $0 \leq x \leq x_1$

$$\begin{aligned}
A_+^{(1)} e^{ik_1^{(1)}x} + B_+^{(1)} e^{-ik_1^{(1)}x} &= e^{ik_1x} - \frac{\mathbf{i}}{K_{\text{eff}}^{(1)} - k_1} \left[T^{(1)} A_+^{(1)} + R^{(1)} A_-^{(1)} \right] \left[e^{ik_1^{(1)}x} - e^{ik_1x} \right] \\
&+ \frac{\mathbf{i}}{K_{\text{eff}}^{(1)} + k_1} \left[T^{(1)} B_+^{(1)} + R^{(1)} B_-^{(1)} \right] \left[e^{-ik_1^{(1)}x} - e^{ik_1x} \right]
\end{aligned} \quad (4.7)$$

for $x_{j-1} \leq x \leq x_j (2 \leq j \leq N)$

$$\begin{aligned}
A_+^{(j)} e^{ik_1^{(j)}x} + B_+^{(j)} e^{-ik_1^{(j)}x} &= e^{ik_1x} - e^{ik_1x} \sum_{m=1}^{j-1} \frac{\mathbf{i}}{K_{\text{eff}}^{(m)} - k_1} \left[T^{(m)} A_+^{(m)} + R^{(m)} A_-^{(m)} \right] \left[e^{i(K_{\text{eff}}^{(m)} - k_1)x_m} - e^{i(K_{\text{eff}}^{(m)} - k_1)x_{m-1}} \right] \\
&+ e^{ik_1x} \sum_{m=1}^{j-1} \frac{\mathbf{i}}{K_{\text{eff}}^{(m)} + k_1} \left[T^{(m)} B_+^{(m)} + R^{(m)} B_-^{(m)} \right] \left[e^{-i(K_{\text{eff}}^{(m)} + k_1)x_m} - e^{-i(K_{\text{eff}}^{(m)} + k_1)x_{m-1}} \right] \\
&- \frac{\mathbf{i}}{K_{\text{eff}}^{(j)} - k_1} \left[T^{(j)} A_+^{(j)} + R^{(j)} A_-^{(j)} \right] \left[e^{ik_1^{(j)}x} - e^{i(K_{\text{eff}}^{(j)} - k_1)x_{j-1}} e^{ik_1x} \right] \\
&+ \frac{\mathbf{i}}{K_{\text{eff}}^{(j)} + k_1} \left[T^{(j)} B_+^{(j)} + R^{(j)} B_-^{(j)} \right] \left[e^{-ik_1^{(j)}x} - e^{-i(K_{\text{eff}}^{(j)} + k_1)x_{j-1}} e^{ik_1x} \right]
\end{aligned} \quad (4.8)$$

for $x_{j-1} \leq x \leq x_j (1 \leq j \leq N - 1)$

$$\begin{aligned}
A_-^{(j)} e^{ik_1^{(j)}x} + B_-^{(j)} e^{-ik_1^{(j)}x} &= -e^{-ik_1x} \sum_{m=j+1}^N \frac{\mathbf{i}}{K_{\text{eff}}^{(m)} + k_1} \left[R^{(m)} A_+^{(m)} + T^{(m)} A_-^{(m)} \right] \left[e^{i(K_{\text{eff}}^{(m)} + k_1)x_m} - e^{i(K_{\text{eff}}^{(m)} + k_1)x_{m-1}} \right] \\
&+ e^{-ik_1x} \sum_{m=j+1}^N \frac{\mathbf{i}}{K_{\text{eff}}^{(m)} - k_1} \left[R^{(m)} B_+^{(m)} + T^{(m)} B_-^{(m)} \right] \left[e^{i(-K_{\text{eff}}^{(m)} + k_1)x_m} - e^{i(-K_{\text{eff}}^{(m)} + k_1)x_{m-1}} \right] \\
&- \frac{\mathbf{i}}{K_{\text{eff}}^{(j)} + k_1} \left[R^{(j)} A_+^{(j)} + T^{(j)} A_-^{(j)} \right] \left[e^{i(K_{\text{eff}}^{(j)} + k_1)x_j} e^{-ik_1x} - e^{iK_{\text{eff}}^{(j)}x} \right] \\
&+ \frac{\mathbf{i}}{K_{\text{eff}}^{(j)} - k_1} \left[R^{(j)} B_+^{(j)} + T^{(j)} B_-^{(j)} \right] \left[e^{i(-K_{\text{eff}}^{(j)} + k_1)x_j} e^{-ik_1x} - e^{-iK_{\text{eff}}^{(j)}x} \right]
\end{aligned} \quad (4.9)$$

for $x_{N-1} \leq x \leq x_N$

$$\begin{aligned}
A_-^{(N)} e^{ik_1^{(N)}x} + B_-^{(N)} e^{-ik_1^{(N)}x} &= -\frac{\mathbf{i}}{K_{\text{eff}}^{(N)} + k_1} \left[R^{(N)} A_+^{(N)} + T^{(N)} A_-^{(N)} \right] \left[e^{i(K_{\text{eff}}^{(N)} + k_1)x_N} e^{-ik_1x} - e^{iK_{\text{eff}}^{(N)}x} \right] \\
&+ \frac{\mathbf{i}}{K_{\text{eff}}^{(N)} - k_1} \left[R^{(N)} B_+^{(N)} + T^{(N)} B_-^{(N)} \right] \left[e^{i(-K_{\text{eff}}^{(N)} + k_1)x_N} e^{-ik_1x} - e^{-iK_{\text{eff}}^{(N)}x} \right]
\end{aligned} \quad (4.10)$$

The only way for Eqs. (4.7–4.10) to hold all together, whatever the value of x , is to cancel the coefficients in front of each of the exponential terms $e^{\pm ik_1^{(j)}x}$ and $e^{\pm ik_1x} (1 \leq j \leq N)$.

Canceling the coefficients associated to $e^{\pm ik_1^{(j)}x} (1 \leq j \leq N)$ provides what is called the Lorentz–Lorenz law [1],

$$A_+^{(j)} + \frac{\mathbf{i}}{K_{\text{eff}}^{(j)} - k_1} \left[T^{(j)} A_+^{(j)} + R^{(j)} A_-^{(j)} \right] = 0, \quad A_-^{(j)} - \frac{\mathbf{i}}{K_{\text{eff}}^{(j)} + k_1} \left[R^{(j)} A_+^{(j)} + T^{(j)} A_-^{(j)} \right] = 0 \quad (4.11)$$

$$B_+^{(j)} - \frac{\mathbf{i}}{K_{\text{eff}}^{(j)} + k_1} \left[T^{(j)} B_+^{(j)} + R^{(j)} B_-^{(j)} \right] = 0, \quad B_-^{(j)} + \frac{\mathbf{i}}{K_{\text{eff}}^{(j)} - k_1} \left[R^{(j)} B_+^{(j)} + T^{(j)} B_-^{(j)} \right] = 0 \quad (4.12)$$

For coherent waves to actually propagate back and forth in each layer j , trivial solutions of both Eqs. (4.11) and (4.12) are forbidden, and the determinants of each set of equations are set to zero, leading to

$$K_{\text{eff}}^{(j)2} = R^{(j)2} - \left(ik_1 + T^{(j)} \right)^2 \quad (4.13)$$

Taking into account Eqs. (4.1) and (4.13) is equivalent to

$$K_{\text{eff}}^{(j)2} = \left[k_1 + \frac{2n_j}{ik_1} f_j(\mathbf{i}, \mathbf{i}) \right]^2 - \left[\frac{2n_j}{ik_1} f_j(\mathbf{i}, -\mathbf{i}) \right]^2 \quad (4.14)$$

which is nothing else but Waterman and Truell's formula [6]. Eq. (4.14) is a second order correction to Foldy's equation [4] that allows the cylinders to overlap. Denying that possibility to the cylinders leads, through Fikioris and Waterman's hole correction, to an implicit relation for the effective wavenumber [7], which has been shown by Linton and Martin to reduce to a different second order correction of Foldy's equation than Eq. (4.14), under the assumption that both the concentration

of scatterers and the n_j/k_1^2 ratio are small [15]. There is, as previously mentioned, little numerical difference between all formulas for low concentrations of not too resonant scatterers [19].

Canceling the coefficients associated to $e^{\pm ik_1 x}$ ($1 \leq j \leq N$) gives what is known as the Theorem of extinction [1]. Canceling the coefficients associated to $e^{ik_1 x}$ and $e^{-ik_1 x}$ in Eqs. (4.7) and (4.10) respectively, when taking into account Eqs. (4.11) and (4.12), leads to

$$\psi_+^{(1)}(x = 0) = A_+^{(1)} + B_+^{(1)} = 1 \tag{4.15}$$

$$\psi_-^{(N)}(x = d) = A_-^{(N)} e^{ik_{eff}^{(N)} d} + B_-^{(N)} e^{-ik_{eff}^{(N)} d} = 0 \tag{4.16}$$

Canceling the coefficients associated to $e^{ik_1 x}$ in Eq. (4.8), whilst still taking into account Eqs. (4.11) and (4.12), leads to ($2 \leq j \leq N$)

$$1 - A_+^{(j)} e^{i \left(K_{eff}^{(j)} - k_1 \right) x_{j-1}} + \sum_{m=1}^{j-1} A_+^{(m)} \left[e^{i \left(K_{eff}^{(m)} - k_1 \right) x_m} - e^{i \left(K_{eff}^{(m)} - k_1 \right) x_{m-1}} \right] - B_+^{(j)} e^{-i \left(K_{eff}^{(j)} + k_1 \right) x_{j-1}} + \sum_{m=1}^{j-1} B_+^{(m)} \left[e^{-i \left(K_{eff}^{(m)} + k_1 \right) x_m} - e^{-i \left(K_{eff}^{(m)} + k_1 \right) x_{m-1}} \right] = 0 \tag{4.17}$$

Index j can be replaced by $j - 1$ in Eq. (4.17) for $2 \leq j - 1 \leq N$ ($3 \leq j \leq N$). This new relation is subtracted from Eq. (4.17) that turns to

$$A_+^{(j-1)} e^{ik_{eff}^{(j-1)} x_{j-1}} + B_+^{(j-1)} e^{-ik_{eff}^{(j-1)} x_{j-1}} = A_+^{(j)} e^{ik_{eff}^{(j)} x_{j-1}} + B_+^{(j)} e^{-ik_{eff}^{(j)} x_{j-1}} \tag{4.18}$$

provided that $3 \leq j \leq N$. Use of Eq. (4.17) with $j = 2$, combined with Eq. (4.15), shows that Eq. (4.18) still holds for $j = 2$, so that Eq. (4.19),

$$A_+^{(j)} e^{ik_{eff}^{(j)} x_j} + B_+^{(j)} e^{-ik_{eff}^{(j)} x_j} = A_+^{(j+1)} e^{ik_{eff}^{(j+1)} x_j} + B_+^{(j+1)} e^{-ik_{eff}^{(j+1)} x_j}, \tag{4.19}$$

holds for $1 \leq j \leq N - 1$. In the same way, canceling the coefficients associated to $e^{-ik_1 x}$ in Eq. (4.9) and using Eq. (4.16) leads to the following equation

$$A_-^{(j)} e^{ik_{eff}^{(j)} x_j} + B_-^{(j)} e^{-ik_{eff}^{(j)} x_j} = A_-^{(j+1)} e^{ik_{eff}^{(j+1)} x_j} + B_-^{(j+1)} e^{-ik_{eff}^{(j+1)} x_j} \tag{4.20}$$

for $1 \leq j \leq N - 1$. Following Twersky [16], the reflected and transmitted waves are defined as $\psi_R(x) = R_{slab} e^{-ik_1 x} = \psi_-^{(1)}(x = 0) e^{-ik_1 x}$ and $\psi_T(x) = T_{slab} e^{ik_1(x-d)} = \psi_+^{(N)}(x = d) e^{ik_1(x-d)}$, so that

$$R_{slab} = \psi_-^{(1)}(x = 0) \quad \text{and} \quad T_{slab} = \psi_+^{(N)}(x = d) \tag{4.21}$$

From Eqs. (4.11) and (4.12), one easily gets

$$A_-^{(j)} = -Q^{(j)} A_+^{(j)} \quad \text{and} \quad B_-^{(j)} = -B_+^{(j)} / Q^{(j)} \tag{4.22}$$

with

$$Q^{(j)} = T^{(j)} + i(k_1 - K_{eff}^{(j)}) / R^{(j)} \tag{4.23}$$

Consequently, it comes from Eqs. ((4.6), (4.15), (4.16), and (4.21)–(4.23))

$$R_{slab} = A_-^{(1)} + B_-^{(1)} = \frac{1}{Q^{(1)}} \left[(1 - Q^{(1)2}) A_+^{(1)} - 1 \right] \tag{4.24}$$

$$T_{slab} = A_+^{(N)} e^{ik_{eff}^{(N)} d} + B_+^{(N)} e^{-ik_{eff}^{(N)} d} = A_+^{(N)} \left(1 - Q^{(N)2} \right) e^{ik_{eff}^{(N)} d} \tag{4.25}$$

The calculation of R_{slab} and T_{slab} depends thus on that of $A_+^{(1)}$ and $A_+^{(N)}$. The N effective wavenumbers are known already (cf. Eq. (4.13)), and $4N$ equations are needed to determine the $4N$ amplitudes ($A_{\pm}^{(j)}, B_{\pm}^{(j)}$). They are given by Eqs. (4.15), (4.16), (4.19), (4.20) and (4.22). Using Eq. (4.22) in order to express the $2N$ amplitudes ($A_-^{(j)}, B_-^{(j)}$) as functions of the $2N$ amplitudes ($A_+^{(j)}, B_+^{(j)}$), one gets a linear set of equations of rank $2N$ in order to calculate the $2N$ unknown amplitudes ($A_+^{(j)}, B_+^{(j)}$). It comes

$$A_+^{(1)} + B_+^{(1)} = 1 \tag{4.26a}$$

$$Q^{(N)} A_+^{(N)} e^{ik_{eff}^{(N)} x_N} + \frac{1}{Q^{(N)}} B_+^{(N)} e^{-ik_{eff}^{(N)} x_N} = 0 \tag{4.26b}$$

$$A_+^{(j)} e^{ik_{eff}^{(j)} x_j} + B_+^{(j)} e^{-ik_{eff}^{(j)} x_j} = A_+^{(j+1)} e^{ik_{eff}^{(j+1)} x_j} + B_+^{(j+1)} e^{-ik_{eff}^{(j+1)} x_j} \tag{4.26c}$$

$$Q^{(j)} A_+^{(j)} e^{ik_{eff}^{(j)} x_j} + \frac{1}{Q^{(j)}} B_+^{(j)} e^{-ik_{eff}^{(j)} x_j} = Q^{(j+1)} A_+^{(j+1)} e^{ik_{eff}^{(j+1)} x_j} + \frac{1}{Q^{(j+1)}} B_+^{(j+1)} e^{-ik_{eff}^{(j+1)} x_j} \tag{4.26d}$$

with $(1 \leq j \leq N - 1)$, and, once Eqs. (4.26) are solved and $A_+^{(1)}, A_+^{(N)}$ determined, both the reflection coefficient and the transmission coefficient can be calculated from Eqs. (4.24) and (4.25). The continuity of pressure and normal displacement at each boundary of the discretized slab is checked in the next section.

5. Boundary conditions at the slab interfaces

Eqs. (4.15) and (4.16) are

$$\psi_+^{(1)}(x=0) = \psi_{inc}(x=0) = 1, \quad \psi_-^{(N)}(x=d) = 0 \quad (5.1)$$

Eq. (5.1) shows the continuity of the pressure waves propagating from the left to the right at $x=0$ as well as that of the waves propagating from the right to the left at $x=x_N=d$. Same way, Eqs. (4.19) and (4.20) take the following form

$$\psi_+^{(j)}(x=x_j) = \psi_+^{(j+1)}(x=x_j) \quad \text{and} \quad \psi_-^{(j)}(x=x_j) = \psi_-^{(j+1)}(x=x_j) \quad (5.2)$$

that is the continuity of the pressure waves propagating from the left to the right, on one hand, and of those propagating from the right to the left on the other hand, at the interface $x=x_j (1 \leq j \leq N-1)$. However, the true boundary conditions do not deal with $\psi_+^{(j)}$ and $\psi_-^{(j)}$ separately but with the $\langle \psi^{(j)} \rangle = \psi_+^{(j)} + \psi_-^{(j)}$ mean fields. They are merely obtained by gathering up Eqs. (4.21), (5.1) and (5.2)

$$\langle \psi^{(1)} \rangle(x=0) = \psi_+^{(1)}(x=0) + \psi_-^{(1)}(x=0) = 1 + R_{slab} = \psi_{inc}(x=0) + \psi_R(x=0) \quad (5.3)$$

$$\langle \psi^{(N)} \rangle(x=d) = \psi_+^{(N)}(x=d) + \psi_-^{(N)}(x=d) = T_{slab} = \psi_T(x=d) \quad (5.4)$$

$$\langle \psi^{(j)} \rangle(x=x_j) = \langle \psi^{(j+1)} \rangle(x=x_j) \quad (1 \leq j \leq N-1) \quad (5.5)$$

The continuity of the mean pressure fields is hence verified at all the interfaces of the discretized slab.

Let us check now the continuity of normal displacement. The effective mass density of the uniform slab number j is defined, according to Eq. (2.3), as

$$\rho_{eff}^{(j)} = \rho_1 \frac{K_{eff}^{(j)} (1 - Q^{(j)})}{k_1 (1 + Q^{(j)})} \quad (5.6)$$

Normal displacement is continuous at the $x=0$ interface if Eq. (5.7) is fulfilled.

$$\frac{1}{\rho_{eff}^{(1)}} \left[\frac{\partial \psi_+^{(1)}}{\partial x} + \frac{\partial \psi_-^{(1)}}{\partial x} \right]_{x=0} = \frac{1}{\rho_1} \left[\frac{\partial \psi_{inc}}{\partial x} + \frac{\partial \psi_R}{\partial x} \right]_{x=0} = \frac{ik_1}{\rho_1} [1 - R_{slab}] \quad (5.7)$$

Using Eqs. (4.6) and (4.24), Eq. (5.7) turns into Eq. (5.8)

$$\frac{K_{eff}^{(1)}}{\rho_{eff}^{(1)}} [A_+^{(1)} - B_+^{(1)} + A_-^{(1)} - B_-^{(1)}] = \frac{k_1}{\rho_1} [1 - A_-^{(1)} - B_-^{(1)}], \quad (5.8)$$

which, with use of Eqs. (4.26a) and (5.6), gives

$$(1 + Q^{(1)}) [A_+^{(1)} - B_+^{(1)} + A_-^{(1)} - B_-^{(1)}] = (1 - Q^{(1)}) [A_+^{(1)} + B_+^{(1)} - A_-^{(1)} - B_-^{(1)}] \quad (5.9)$$

It is now easy to verify, with the help of Eq. (4.22), that Eq. (5.9) is fulfilled, and so is Eq. (5.7).

Normal displacement is continuous at the $x=d$ interface if Eq. (5.10) is fulfilled

$$\frac{1}{\rho_{eff}^{(N)}} \left[\frac{\partial \psi_+^{(N)}}{\partial x} + \frac{\partial \psi_-^{(N)}}{\partial x} \right]_{x=d} = \frac{1}{\rho_1} \left[\frac{\partial \psi_T}{\partial x} \right]_{x=d} = \frac{ik_1}{\rho_1} T_{slab} \quad (5.10)$$

or (cf. Eqs. (4.6), (4.25) and (5.6))

$$(1 + Q^{(N)}) [A_+^{(N)} e^{ik_{eff}^{(N)} d} - B_+^{(N)} e^{-ik_{eff}^{(N)} d} + A_-^{(N)} e^{ik_{eff}^{(N)} d} - B_-^{(N)} e^{-ik_{eff}^{(N)} d}] = (1 - Q^{(N)}) [A_+^{(N)} e^{ik_{eff}^{(N)} d} + B_+^{(N)} e^{-ik_{eff}^{(N)} d}] \quad (5.11)$$

With use of Eqs. (4.22) and (5.11) reduces to

$$Q^{(N)} A_+^{(N)} e^{ik_{eff}^{(N)} d} + \frac{1}{Q^{(N)}} B_+^{(N)} e^{-ik_{eff}^{(N)} d} = 0 \quad (5.12)$$

which is nothing else but Eq. (4.26b). Continuity of normal displacement at the $x=d$ interface is thus ensured.

Continuity of normal displacement at each interface $x=x_j (1 \leq j \leq N-1)$

$$\frac{1}{\rho_{eff}^{(j)}} \left[\frac{\partial \psi_+^{(j)}}{\partial x} + \frac{\partial \psi_-^{(j)}}{\partial x} \right]_{x=x_j} = \frac{1}{\rho_{eff}^{(j+1)}} \left[\frac{\partial \psi_+^{(j+1)}}{\partial x} + \frac{\partial \psi_-^{(j+1)}}{\partial x} \right]_{x=x_j} \quad (5.13)$$

is no more difficult to check. Use of Eqs. (4.6) and (5.6) gives

$$\begin{aligned} & \left(1 + Q^{(j)}\right)\left(1 - Q^{(j+1)}\right) \left[A_+^{(j)} e^{iK_{eff}^{(j)} x_j} - B_+^{(j)} e^{-iK_{eff}^{(j)} x_j} + A_-^{(j)} e^{iK_{eff}^{(j)} x_j} - B_-^{(j)} e^{-iK_{eff}^{(j)} x_j} \right] \\ &= \left(1 + Q^{(j+1)}\right)\left(1 - Q^{(j)}\right) \left[A_+^{(j+1)} e^{iK_{eff}^{(j+1)} x_j} - B_+^{(j+1)} e^{-iK_{eff}^{(j+1)} x_j} + A_-^{(j+1)} e^{iK_{eff}^{(j+1)} x_j} - B_-^{(j+1)} e^{-iK_{eff}^{(j+1)} x_j} \right]. \end{aligned} \tag{5.14}$$

From Eq. (4.22), one gets

$$\left(1 + Q^{(j)}\right) \left[A_+^{(j)} e^{iK_{eff}^{(j)} x_j} + \frac{B_+^{(j)}}{Q^{(j)}} e^{-iK_{eff}^{(j)} x_j} \right] = \left(1 + Q^{(j+1)}\right) \left[A_+^{(j+1)} e^{iK_{eff}^{(j+1)} x_j} + \frac{B_+^{(j+1)}}{Q^{(j+1)}} e^{-iK_{eff}^{(j+1)} x_j} \right] \tag{5.15}$$

which is the sum of Eqs. (4.26c) and (4.26d). So, the continuity of normal displacement at each interface $x = x_j (1 \leq j \leq N - 1)$ is also proved. It is important here to point out that the effective mass density (cf. Eqs. (2.3) and (5.6)) defined in Section 2 is the only one that links the acoustic displacement mean field to the pressure one in such a way that the continuity of normal displacement at the interface between two different uniform slabs is guaranteed.

6. The reflection and transmission coefficients as debye's series

The goal of this section is to express the reflection and transmission coefficients of the discretized slab as series involving the reflection–transmission coefficients of each interface of the discretized slab, same way as in Eqs. (1.1) and (1.2). Such explicit formulas indeed are much easier to handle than Eqs. (4.24) and (4.25) that impose the resolution of the linear set of equations Eqs. (4.26): solving Eqs. (4.26), of rank $2N$, becomes time-consuming with the increase of N .

Of course, there are other methods, based on transfer matrices, which can be used to express reflection and transmission with regard to the reflection–transmission coefficients of each interface. The ones tested give exactly the same results with comparable computation times. Debye's series are presented here, this is a choice, because they provide an analytical and explicit generalisation of Eqs. (1.1) and (1.2).

The reflection–transmission coefficients at the j th interface ($1 \leq j \leq N + 1$) are found, from the boundary conditions of the previous section, as

$$R_{j-1j} = -R_{jj-1} = \frac{Z_j - Z_{j-1}}{Z_j + Z_{j-1}}, \quad T_{j-1j} = \frac{2Z_j}{Z_j + Z_{j-1}}, \quad T_{j-1j} = \frac{2Z_{j-1}}{Z_j + Z_{j-1}} \tag{6.1}$$

with $Z_0 = Z_{N+1} = \rho_1 \omega / k_1$ and ($1 \leq j \leq N$)

$$Z_j = \rho_{eff}^{(j)} \frac{\omega}{K_{eff}^{(j)}} = Z_0 \frac{1 - Q^{(j)}}{1 + Q^{(j)}} \tag{6.2}$$

As expected, these coefficients take the same form as the usual reflection–transmission coefficients at the interface between two fluids [27].

In order to find the expressions of R_{slab} and T_{slab} in terms of the local coefficients of Eq. (6.1), let us consider first the discretized slab as composed of the single layer $0 \leq x \leq x_1$ bounded by the homogeneous fluid [$x \leq 0$] and the multilayer [$x \geq x_1$]. The reflection coefficient of the slab can thus be written (cf. Eq. (1.1)) as

$$R_{slab} = R_{01} + \frac{T_{01} R_{slab}^{(1)} T_{10} e^{2iK_{eff}^{(1)} x_1}}{1 - R_{10} R_{slab}^{(1)} e^{2iK_{eff}^{(1)} x_1}} \tag{6.3}$$

where $R_{slab}^{(1)}$ characterizes the reflection by the multilayer [$x \geq x_1$]. Of course, $R_{slab}^{(1)}$ is unknown at this step of the calculation. However, it can be expressed in the same way as R_{slab} , by considering the multilayer [$x \geq x_1$] as composed of the single layer $x_1 \leq x \leq x_2$, bounded by the layer $0 \leq x \leq x_1$ on its left, and by the multilayer [$x \geq x_2$] on its right,

$$R_{slab}^{(1)} = R_{12} + \frac{T_{12} R_{slab}^{(2)} T_{21} e^{2iK_{eff}^{(2)} (x_2 - x_1)}}{1 - R_{21} R_{slab}^{(2)} e^{2iK_{eff}^{(2)} (x_2 - x_1)}} \tag{6.4}$$

with $R_{slab}^{(2)}$ the reflection coefficient of the multilayer [$x \geq x_2$]. The same process is iterated until the last interface $x = d$ is reached. Thus, the reflection coefficient $R_{slab}^{(j)}$ depends on the next one $R_{slab}^{(j+1)}$ so that $R_{slab}^{(j)}$ is well defined provided $R_{slab}^{(j+1)}$ is known. At the last interface $x = d$,

$$R_{slab}^{(N)} = R_{NN+1} \tag{6.5}$$

As $R_{slab}^{(N)}$ is known, it is possible to calculate $R_{slab}^{(N-1)}$ and, step by step, all the other coefficients back to $R_{slab}^{(1)}$. It follows that R_{slab} is given by Eq. (6.3) along with a relation of recurrence,

$$R_{slab}^{(j)} = R_{jj+1} + \frac{T_{jj+1}R_{slab}^{(j+1)}T_{j+1j}e^{2ik_{eff}^{(j)}(x_{j+1}-x_j)}}{1 - R_{j+1j}R_{slab}^{(j+1)}e^{2ik_{eff}^{(j)}(x_{j+1}-x_j)}} \quad (1 \leq j \leq N - 1) \tag{6.6}$$

which is initialized by Eq. (6.5) for $j = N$.

Following the same procedure, T_{slab} is given by (cf. Eq. (1.2))

$$T_{slab} = \frac{T_{01}T_{slab}^{(1)}e^{ik_{eff}^{(1)}x_1}}{1 - R_{10}R_{slab}^{(1)}e^{2ik_{eff}^{(1)}x_1}} \tag{6.7}$$

where $T_{slab}^{(1)}$ is the transmission coefficient by the multilayer $[x \geq x_1]$. $T_{slab}^{(1)}$ can be expressed with regard to the transmission coefficient by the multilayer $[x \geq x_2]$, $T_{slab}^{(2)}$, and so on. The relation of recurrence to be used is then

$$T_{slab}^{(j)} = \frac{T_{jj+1}T_{slab}^{(j+1)}e^{ik_{eff}^{(j+1)}(x_{j+1}-x_j)}}{1 - R_{j+1j}R_{slab}^{(j+1)}e^{2ik_{eff}^{(j+1)}(x_{j+1}-x_j)}}, \quad (1 \leq j \leq N - 1) \quad \text{and} \quad T_{slab}^{(N)} = T_{NN+1} \tag{6.8}$$

This way, both the reflection and transmission coefficients are written in a compact form that is very useful for numerical calculations. Each denominator in Eqs. (6.3), (6.6), (6.7) and (6.8) can be expanded into geometrical series that allow in turn the expression of R_{slab} and T_{slab} as series, which are known as the Debye's series in the framework of the Resonant Scattering Theory [32]. These series account for all the reflections and refractions inside the discretized slab, which is considered as an interferometer.

7. The WKB method applied to the smooth-varying slab

Once again, the starting point is the set of coupled integral equations Eq. (3.10). The variations of $n(x)$, $R(x)$, and $T(x)$ are supposed smooth, and

$$n'(x) \ll n(x), \quad |R'(x)| \ll |R(x)| \quad \text{and} \quad |T'(x)| \ll |T(x)| \tag{7.1}$$

In other words, both the concentration and size of the cylinders are slow varying parameters. When differentiated, Eq. (3.10) become

$$\psi'_+(x) = [ik_1 + n(x)T(x)]\psi_+(x) + n(x)R(x)\psi_-(x) \tag{7.2a}$$

$$\psi'_-(x) = -[ik_1 + n(x)T(x)]\psi_-(x) - n(x)R(x)\psi_+(x) \tag{7.2b}$$

Taking into account the assumptions in Eq. (7.1), the differentiation of Eqs. (7.2) leads to

$$\psi''_{\pm}(x) + K_{eff}^2(x)\psi_{\pm}(x) \cong 0 \tag{7.3}$$

with

$$K_{eff}^2(x) = n^2(x)R^2(x) - [ik_1 + n(x)T(x)]^2 \tag{7.4}$$

where $R(x)$ and $T(x)$ are defined in Eq. (3.11). It must be noted here that the backscattering $f(\hat{i}, -\hat{i}; x)$ and forwardscattering $f(\hat{i}, \hat{i}; x)$ functions depend on the x -coordinate because they depend on the radius (size) $a(x)$ of the cylinders. According to Eqs. (4.1), (4.13) and (4.14), Eq. (7.4) is clearly that of Waterman and Truell [6] for a concentration and a size of the cylinders depending on the x -coordinate. After Eq. (7.1), it follows that

$$|K'_{eff}(x)| \ll |K_{eff}(x)| \tag{7.5}$$

which is the reason why the WKB method can be used in that case.

The WKB solution of Eq. (7.3) is very well known [27]

$$\psi_{\pm}(x) = \frac{A_{\pm}}{\sqrt{K_{eff}(x)}} e^{i \int_0^x K_{eff}(x_s) dx_s} + \frac{B_{\pm}}{\sqrt{K_{eff}(x)}} e^{-i \int_0^x K_{eff}(x_s) dx_s} \tag{7.6}$$

with A_{\pm} and B_{\pm} the unknown constants. The only way to determine them is to use the boundary conditions at $x = 0$ and $x = d$. In order to do so, the following notations are introduced

$$n(x = 0) = n_0, \quad n(x = d) = n_d, \quad K_{eff}(x = 0) = K_{eff}^{(0)}, \quad K_{eff}(x = d) = K_{eff}^{(d)} \tag{7.7}$$

$$\langle K_{eff} \rangle = \frac{1}{d} \int_0^d K_{eff}(x_s) dx_s \tag{7.8}$$

with $\langle K_{eff} \rangle$ the average effective wavenumber of the varying slab.

Continuity of pressure reads

$$\psi_+(0) + \psi_-(0) = 1 + R_{slab} \quad \text{and} \quad \psi_+(d) + \psi_-(d) = T_{slab} \quad (7.9)$$

with

$$\psi_-(0) = R_{slab} \quad \text{and} \quad \psi_+(d) = T_{slab} \quad (7.10)$$

It follows that

$$\psi_+(0) = 1 \quad \text{and} \quad \psi_-(d) = 0 \quad (7.11)$$

Inserting Eq. (7.6) into Eq. (7.11) gives

$$A_+ + B_+ = \sqrt{K_{eff}^{(0)}}, \quad A_- e^{i(K_{eff})d} + B_- e^{-i(K_{eff})d} = 0 \quad (7.12)$$

Continuity of normal displacement reads

$$\frac{1}{\rho_{eff}^{(0)}} \left[\frac{\partial \psi_+}{\partial x}(0) + \frac{\partial \psi_-}{\partial x}(0) \right] = \frac{1}{\rho_1} \left[\frac{\partial \psi_{inc}}{\partial x}(0) + \frac{\partial \psi_R}{\partial x}(0) \right] \quad (7.13a)$$

$$\frac{1}{\rho_{eff}^{(d)}} \left[\frac{\partial \psi_+}{\partial x}(d) + \frac{\partial \psi_-}{\partial x}(d) \right] = \frac{1}{\rho_1} \left[\frac{\partial \psi_T}{\partial x}(d) \right] \quad (7.13b)$$

where $\rho_{eff}^{(0)} = \rho_{eff}(x=0)$ and $\rho_{eff}^{(d)} = \rho_{eff}(x=d)$ are the effective mass densities at the beginning and at the end of the slowly-varying slab. The x -dependence of the effective mass density is quite naturally the generalization of Eq. (2.3) to the continuous counter-part of Eq. (5.6),

$$\rho_{eff}(x) = \rho_1 \frac{K_{eff}(x) (1 - Q(x))}{k_1 (1 + Q(x))} \quad (7.14)$$

with (cf. Eqs. (4.1) and (4.23))

$$Q(x) = \frac{n(x)T(x) + i(k_1 - K_{eff}(x))}{n(x)R(x)} \quad (7.15)$$

The impedance ratios

$$\tau_0 = \frac{\rho_{eff}^{(0)} k_1}{\rho_1 K_{eff}^{(0)}} = \frac{1 - Q_0}{1 + Q_0} \quad \text{and} \quad \tau_d = \frac{\rho_{eff}^{(d)} k_1}{\rho_1 K_{eff}^{(d)}} = \frac{1 - Q_d}{1 + Q_d} \quad (7.16)$$

are also introduced, with $Q_0 = Q(x=0)$ and $Q_d = Q(x=d)$.

In the field of the WKB approximation, k_1 is assumed to be large, and, as $|K_{eff}|$ is of the same order as k_1 , one has

$$\frac{\partial}{\partial x} \left[\frac{e^{\pm i \int_0^x K_{eff}(x_s) dx_s}}{\sqrt{K_{eff}(x)}} \right] = \sqrt{K_{eff}(x)} \left[\pm i - \frac{1}{2K_{eff}^2(x)} \right] e^{\pm i \int_0^x K_{eff}(x_s) dx_s} \cong \pm i \sqrt{K_{eff}(x)} e^{\pm i \int_0^x K_{eff}(x_s) dx_s} \quad (7.17)$$

As a consequence, once Eq. (7.6) is introduced in Eq. (7.13), and Eq. (7.17) taken into account, one gets

$$(1 + Q_0)A_+ - (1 + Q_0)B_+ + 2A_- - 2Q_0B_- = \sqrt{K_{eff}^{(0)}}(1 - Q_0) \quad (7.18a)$$

$$2Q_d A_+ e^{i(K_{eff})d} - 2B_+ e^{-i(K_{eff})d} + (1 + Q_d)A_- e^{i(K_{eff})d} - (1 + Q_d)B_- e^{-i(K_{eff})d} = 0 \quad (7.18b)$$

The solution of the set of linear equations Eqs. (7.12 and 7.18) is given by

$$\frac{A_+}{\sqrt{K_{eff}^{(0)}}} = \frac{1 - (1 + Q_d - Q_0)e^{2i(K_{eff})d}}{(1 - e^{2i(K_{eff})d})(1 - Q_0Q_d e^{2i(K_{eff})d})}, \quad \frac{A_-}{\sqrt{K_{eff}^{(0)}}} = \frac{-Q_0 + Q_d e^{2i(K_{eff})d}}{(1 - e^{2i(K_{eff})d})(1 - Q_0Q_d e^{2i(K_{eff})d})} \quad (7.19a)$$

$$\frac{B_+}{\sqrt{K_{eff}^{(0)}}} = \frac{Q_d - Q_0 - Q_0Q_d(1 - e^{2i(K_{eff})d})}{(1 - e^{2i(K_{eff})d})(1 - Q_0Q_d e^{2i(K_{eff})d})} e^{2i(K_{eff})d}, \quad \frac{B_-}{\sqrt{K_{eff}^{(0)}}} = \frac{[Q_0 - Q_d e^{2i(K_{eff})d}] e^{2i(K_{eff})d}}{(1 - e^{2i(K_{eff})d})(1 - Q_0Q_d e^{2i(K_{eff})d})} \quad (7.19b)$$

Finally, the reflection and transmission coefficients can be calculated from Eqs. (7.6) and (7.10),

$$R_{slab} = \frac{-Q_0 + Q_d e^{2i(K_{eff})d}}{1 - Q_0Q_d e^{2i(K_{eff})d}} = \frac{(\tau_0 - 1)(1 + \tau_d) + (\tau_0 + 1)(1 - \tau_d)e^{2i(K_{eff})d}}{(\tau_0 + 1)(1 + \tau_d) + (\tau_0 - 1)(1 - \tau_d)e^{2i(K_{eff})d}} \quad (7.20a)$$

$$T_{slab} = \frac{\sqrt{K_{eff}^{(0)}} (1 + Q_d)(1 - Q_0)e^{i(K_{eff})d}}{\sqrt{K_{eff}^{(d)}} (1 - Q_0Q_d e^{2i(K_{eff})d})} = \frac{\sqrt{K_{eff}^{(0)}}}{\sqrt{K_{eff}^{(d)}}} \frac{4\tau_0 e^{i(K_{eff})d}}{(\tau_0 + 1)(1 + \tau_d) + (\tau_0 - 1)(1 - \tau_d)e^{2i(K_{eff})d}} \quad (7.20b)$$

In the case where the features of the slab are the same at the beginning and at the end, i.e. $n_d = n_0, K_{eff}^{(d)} = K_{eff}^{(0)}, \rho_{eff}^{(d)} = \rho_{eff}^{(0)}$ and $Q_d = Q_0$, Eq. (7.20) come down to

$$R_{slab} = \frac{(\tau_0^2 - 1) + (1 - \tau_0^2)e^{2i\langle K_{eff} \rangle d}}{(1 + \tau_0)^2 - (1 - \tau_0)^2 e^{2i\langle K_{eff} \rangle d}}, \quad T_{slab} = \frac{4\tau_0 e^{i\langle K_{eff} \rangle d}}{(1 + \tau_0)^2 - (1 - \tau_0)^2 e^{2i\langle K_{eff} \rangle d}} \tag{7.21}$$

These expressions are formally identical to those given by Twersky in Ref. [16] (cf. Eqs (3.14)) for a uniform slab. The difference lies in the introduction of $\langle K_{eff} \rangle$ instead of K_{eff} , as the latter is not a constant. The varying slab is thus equivalent to a uniform slab characterized by the impedance ratio τ_0 at the interfaces and by the average effective wavenumber $\langle K_{eff} \rangle$ that describes the propagation of the average coherent wave.

When the characteristics at the two interfaces of the slab are different, two impedance ratios τ_0 and τ_d are required, and the expressions of the reflection and transmission coefficients are a little bit more complicated (cf. Eqs. (7.20)). In this case, the reflection and transmission coefficients look like those of a fluid plate surrounded by two different homogeneous fluids (cf. Ref. [27] p. 28).

Let us consider now the reflection–refraction coefficients at the two interfaces of the slab (the homogeneous fluids $[x \leq 0]$ and $[x \geq d]$ are labeled 0 and d , the varying slab is labeled 1)

$$R_{01} = -R_{10} = \frac{\tau_0 - 1}{1 + \tau_0}, \quad T_{01} = \frac{2\tau_0}{1 + \tau_0} \quad \text{and} \quad T_{10} = \frac{2}{1 + \tau_0} \tag{7.22a}$$

$$R_{1d} = -R_{d1} = \frac{\tau_d - 1}{1 + \tau_d}, \quad T_{1d} = \frac{2\tau_d}{1 + \tau_d} \quad \text{and} \quad T_{d1} = \frac{2}{1 + \tau_d} \tag{7.22b}$$

The reflection and transmission coefficients in Eq. (7.20) can be written as

$$R_{slab} = R_{01} + \frac{T_{01}R_{1d}T_{10}e^{2i\langle K_{eff} \rangle d}}{1 - R_{10}R_{1d}e^{2i\langle K_{eff} \rangle d}}, \quad T_{slab} = \frac{T_{01}T_{1d}e^{i\langle K_{eff} \rangle d}}{1 - R_{10}R_{1d}e^{2i\langle K_{eff} \rangle d}} \tag{7.23}$$

The varying slab can still be considered as an interferometer.

As discussed in the introduction, the impedance ratios τ_0 and τ_d are close to unity at low concentration, so that $R_{01} \cong R_{1d} \cong 0, T_{01} \cong T_{1d} \cong 1$ (cf. Eqs. (7.22)), and $T_{slab} \cong e^{i\langle K_{eff} \rangle d}$ (cf. Eq. (7.23)). This means that transmission experiments can bring no information on $K_{eff}(x)$, but only on its average $\langle K_{eff} \rangle$. Two different varying-slabs, with $K_{eff}^{(1)}(x) \neq K_{eff}^{(2)}(x)$, can give rise to the same average transmitted field, provided that $\langle K_{eff}^{(1)} \rangle = \langle K_{eff}^{(2)} \rangle$. It seems thus rather hopeless to try and identify the profile $(n(x), R(x), T(x))$ of a varying-slab with the help of such a theory.

8. Numerical results

Computations are performed for a space-varying slab characterized by

$$n(x) = \begin{cases} n_{max}e^{-(x-d/2)^2/\sigma^2} & 0 \leq x \leq d \\ 0 & \text{otherwise} \end{cases} \quad \text{with} \quad \sigma^2 = \left(\frac{d}{2}\right)^2 / \ln\left(\frac{n_{max}}{n_{min}}\right) \tag{8.1}$$

and $a(x) = 1$ mm the radius of all cylinders. In Eq. (8.1), $n_{max} = 10^4/\text{m}^2$ and $n_{min} = n_{max}/3$ are, respectively, the maximum and minimum numbers of steel cylinders per unit surface. Eq. (8.1) describes a truncated Gaussian function for which $n(d/2) = n_{max}$ and $n(0) = n(d) = n_{min}$, as shown in Fig. 5. The thickness of the slab is $d = 0.1$ m. As the size of the cylinders is constant all over the slab, so are the forward and backward scattering amplitudes $f(\hat{i}, \pm\hat{i})$. Steel is characterized by its den-

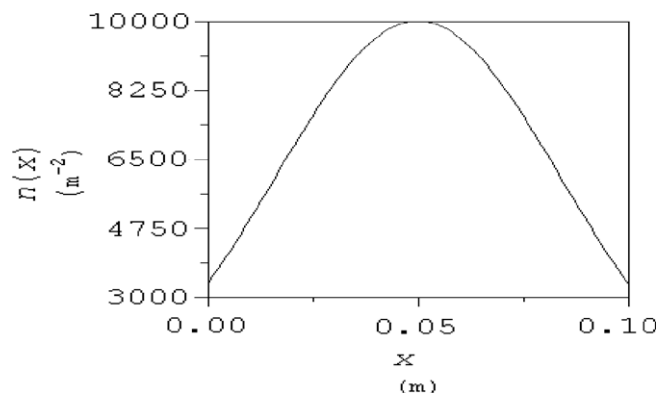


Fig. 5. Average number of steel cylinders per square meter in the thickness of the slab: $n(x)$ is the truncated Gauss function defined in Eq. (8.1).

sity $\rho_s = 7916 \text{ kg/m}^3$, the velocity of the longitudinal waves $c_L = 6000 \text{ m/s}$, and that of the shear waves $c_T = 3100 \text{ m/s}$. The cylinders are immersed in water, characterized by its density $\rho_1 = 1000 \text{ kg/m}^3$ and the velocity of sound $c_1 = 1470 \text{ m/s}$.

First, the space-varying slab is discretized into N layers of thickness $e = d/N$. The reflection and transmission coefficients are then calculated from Eqs. (4.24) and (4.25) after inversion of the linear set of equations (Eqs. (4.26)). The order of convergence is $N = 10$ for the transmission coefficient, while it is equal to 321 for the reflection coefficient. Once the convergence is assured, the moduli of the two Fresnel coefficients are plotted in Figs. 6 and 7 versus the reduced frequency $k_1 a$. In order to understand the difference between the two convergence orders, the reflection coefficient is plotted in Fig. 8 for $N = 70$. Compared to Fig. 6a, periodically spaced spurious peaks are observed at reduced frequencies $k_1 a = 2.2, k_1 a = 4.4, k_1 a = 6.6$ and $k_1 a = 8.8$. They correspond to the first four resonances of a single layer ($1 \leq n \leq 4$):

$$(\lambda_{\text{eff}} \simeq \lambda), n\lambda_{\text{eff}}/2 = e \iff k_1 a \simeq n(N\pi a/d). \tag{8.2}$$

In Eq. (8.2), λ_{eff} is the wavelength of the coherent wave in a layer, which, while depending on that layer, is nonetheless quite close to the wavelength λ in water. Such spurious resonances appear, whatever the value of N , but they are shifted towards higher frequencies as N increases, as shown in Eq. (8.2). For $N = 320$, the first one occurs at $k_1 a = 10.005$, so that it is out of the frequency window of Fig. 6a. In other words, the convergence order for the reflection coefficient depends on the frequency range investigated. It would be $N = 640$ for the frequency range $0 \leq k_1 a \leq 20$. The reason why such spurious resonances are not visible on the plots of the transmission coefficient modulus is not quite clear. It is likely that the interferences in the transmission process involve the coherent waves in all the layers, while only those in the very first layers, which are less absorbing than the middle ones, do contribute to the interferences in the reflection process. More accurately, as the concentration of scatterers varies slowly from one layer to its neighbor, so does the effective wavelength; the interferences are only weakly destroyed from one layer to the other but can be cancelled when all the layers are involved due to cumulative effects.

The reflection and transmission coefficients are calculated much faster from the Debye's series in Eqs. (6.3) and (6.8). The curves obtained are exactly the same as that plotted in Figs. 6–8, meaning that the spurious peaks are actually due to single

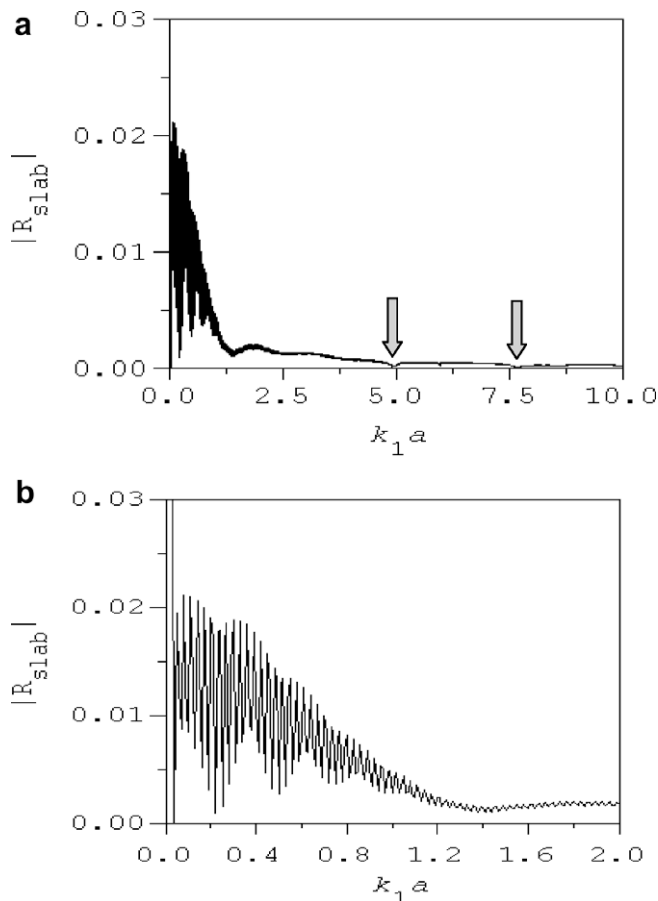


Fig. 6. (a) Modulus of the reflection coefficient of the space-varying slab obtained with $N \geq 321$. Arrows indicate the resonance frequencies of the steel cylinders and (b) same as (a) for $0 \leq k_1 a \leq 2$.

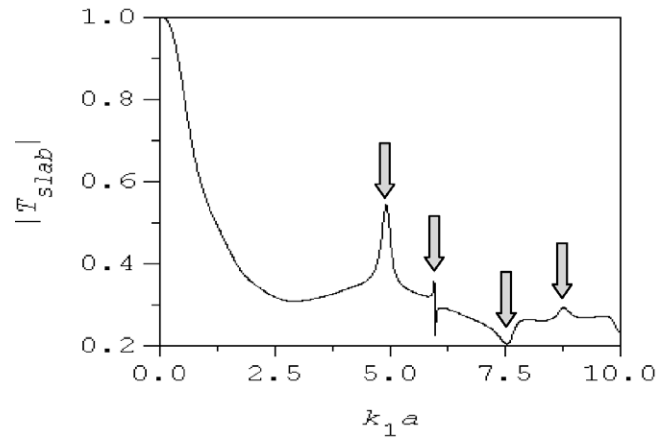


Fig. 7. Modulus of the transmission coefficient of the space-varying slab obtained with $N \geq 321$. Arrows indicate the resonance frequencies of the steel cylinders.

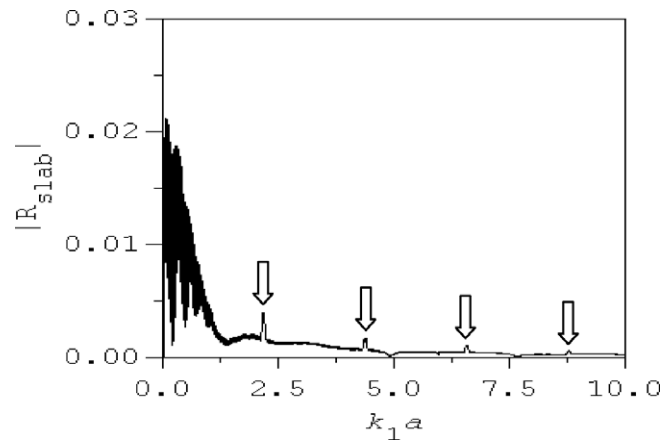


Fig. 8. Modulus of the reflection coefficient of the space-varying slab obtained with $N = 70$. Arrows indicate the spurious peaks associated to resonances of the uniform sub-layers.

layer resonances, not to an ill-conditioned computation. This result proves also, if necessary, that both the mass densities and the boundary conditions, defined in Section 6 and used in the calculation of the Debye's series, are correct.

Use of the even faster WKB method (Eq. (7.21)) leads to the same results than that plotted in Figs. 6 and 7. This shows that the WKB method is relevant, even though the distribution in Fig. 5 is not as slow-varying as the first condition in Eq. (7.1) would require ($|n'(x)/n(x)|$ reaches as much as 40 on both sides of the slab).

In order to get still shorter computation times, consider now a uniform slab, characterized only by the average number of cylinders:

$$\langle n \rangle = \frac{1}{d} \int_0^d n(x_s) dx_s \quad (8.3)$$

which, in the case considered here, is around 7286 m^{-2} . Is that new-defined slab equivalent to the space-varying one? The coherent waves in that slab propagate with a wavenumber $\langle K_{eff} \rangle$ given by Eq. (8.4)

$$\langle K_{eff} \rangle^2 \cong \left[k_1 + \frac{2\langle n \rangle}{ik_1} f(\hat{\mathbf{i}}, \hat{\mathbf{i}}) \right]^2 - \left[\frac{2\langle n \rangle}{ik_1} f(\hat{\mathbf{i}}, -\hat{\mathbf{i}}) \right]^2 \quad (8.4)$$

and its mass density is supposed to be

$$\rho_{eff} \cong \rho_1 \frac{\langle K_{eff} \rangle}{k_1} \frac{1 - \langle Q \rangle}{1 + \langle Q \rangle}, \quad \langle Q \rangle \cong \frac{\frac{2\langle n \rangle}{k_1} f(\hat{\mathbf{i}}, \hat{\mathbf{i}}) + i(k_1 - \langle K_{eff} \rangle)}{\frac{2\langle n \rangle}{k_1} f(\hat{\mathbf{i}}, -\hat{\mathbf{i}})} \quad (8.5)$$

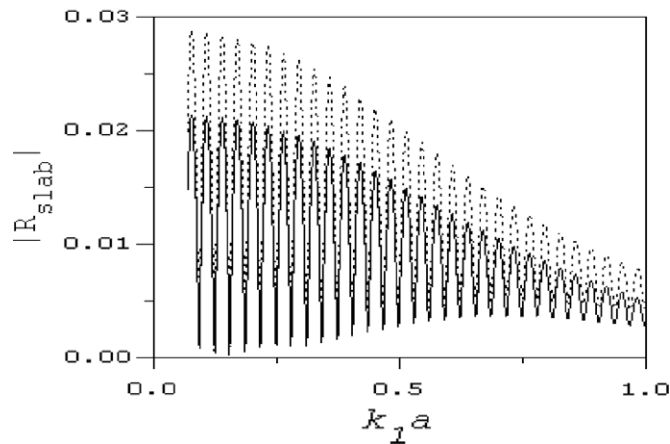


Fig. 9. Modulus of the reflection coefficient of the space varying slab. Lower curve: exact value obtained for $N \geq 321$. Upper curve: approximate value corresponding to a single uniform slab characterized by the average number $\langle n \rangle$ of cylinders as defined in Eq. (8.3).

Its transmission and reflection coefficients can be calculated therefore. The modulus of the transmission coefficient obtained is pretty much the same than that plotted in Fig. 7, but Fig. 9 shows that the reflection coefficient is larger than that of the original space-varying slab. The average effective wavenumber $\langle K_{eff} \rangle$ is well approximated from Eq. (8.4), which is the reason why the oscillations of the two reflection coefficients are practically in phase. Consequently, it is the effective masse density ρ_{eff} given by Eq. (8.5) that is not correct. As shown by the WKB method, it is the effective masse densities $\rho_{eff}^{(0)}$ and $\rho_{eff}^{(d)}$ at the beginning and at the end of the varying slab which must be taken into account. In our case, ρ_{eff} given by Eq. (8.5) overestimates the effective masse density $\rho_{eff}^{(0)} = \rho_{eff}^{(d)}$.

9. Conclusion

Three different expressions have been found for the reflection and transmission coefficients of a space-varying slab at large frequency and low concentration of scatterers. The first two involve the discretization of the properties of the slab. One is obtained after inversion of a linear set of equations of rank $2N$, with N the number of layers introduced by the discretization. The other is the expression of the reflection and transmission coefficients as Debye's series, which are less time consuming. The third expression follows from the use of the WKB Method. All three of them give the same numerical results for a smooth space-varying slab. The three most important results are: (1) Use of the WKB method is relevant for the study of the propagation of coherent waves through a smooth space-varying slab. (2) The method of discretization is efficient insofar as the discretization order is carefully chosen. (3) Once the effective mass density is defined correctly, the boundary conditions, at the interface between a homogeneous fluid and an effective medium, as well as between two different effective media are fulfilled. These are the continuity of pressure and of normal displacement.

References

- [1] L. Tsang, J. Au Kong, Scattering of Electromagnetic Waves – Advanced Topics, Wiley Series in Remote Sensing, John Wiley & Sons, Inc., 2001, ISBN 0-471-38801-7.
- [2] P. Martin, MULTIPLE SCATTERING, Interaction of Time-Harmonic Waves with N Obstacles, Cambridge University Press, 2006, ISBN 0-521-86554-9.
- [3] V. Twersky, On propagation in random media of discrete scatterers, Proc. Am. Math. Soc. Symp. Stochas. Proc. Math. Phys. Eng. 16 (1964) 84–116.
- [4] L.L. Foldy, The multiple scattering of waves. Part I: general theory of isotropic scattering by randomly distributed scatterers, Phys. Rev. 67 (1945) 107–119.
- [5] M. Lax, Multiple scattering of waves. Part II: the effective field in dense systems, Phys. Rev. 85 (1952) 621–629.
- [6] P.C. Waterman, R. Truel, Multiple scattering of waves, J. Math. Phys. 2 (1961) 512–537.
- [7] J.G. Fikioris, P.C. Waterman, Multiple scattering of waves. Part II: hole corrections' in the scalar case, J. Math. Phys. 5 (1964) 1413–1420.
- [8] J.B. Keller, Stochastic equations and wave propagation in random media, in: Proceedings of the 16th Symposium on Applied Mathematics, American Mathematical Society, New York, 1964, pp. 145–179.
- [9] P. Lloyd, M.V. Berry, Wave propagation through an assembly of spheres IV. Relations between different multiple scattering theories, Proc. Phys. Soc. Lond. 91 (1967) 678–688.
- [10] S.K. Bose, A.K. Mal, Longitudinal shear waves in a fiber-reinforced composite, Int. J. Solids Struct. 9 (1973) 1075–1085.
- [11] F.E. Stanke, G.S. Kino, A unified theory for elastic wave propagation in polycrystalline materials, J. Acoust. Soc. Am. 75 (1984) 665–681.
- [12] V.K. Varadan, Y. Ma, V.V. Varadan, Multiple scattering of compressional and shear waves by fiber-reinforced composite materials, J. Acoust. Soc. Am. 80 (1) (1986) 333–339.
- [13] R.B. Yang, A.K. Mal, Multiple scattering of elastic waves in a fiber-reinforced composite, J. Mech. Phys. Solids 42 (12) (1994) 1945–1968.
- [14] S.K. Kanaun, V.M. Levin, Effective medium method in the problem of axial elastic shear wave propagation through fiber composites, Int. J. Solids Struct. 40 (2003) 4859–4878.
- [15] C.M. Linton, P.A. Martin, Multiple scattering by random configurations of circular cylinders: second-order corrections for the effective wavenumber, J. Acoust. Soc. Am. 117 (6) (2005) 3413–3423.
- [16] V. Twersky, On scattering of waves by random distributions. I. Free-space scatterer formalism, J. Math. Phys. 3 (4) (1962) 700–715.

- [17] V. Twersky, On scattering of waves by random distribution. II. Two-space scatterer formalism, *J. Math. Phys.* 3 (4) (1962) 724–734.
- [18] J. Groenenboom, R. Snieder, Attenuation dispersion and anisotropy by multiple scattering of transmitted waves through distributions of scatterers region, *J. Acoust. Soc. Am.* 98 (1995) 3482–3492.
- [19] P.Y. Le Bas, F. Luppé, J.M. Conoir, Reflection and transmission by randomly spaced elastic cylinders in a fluid slab-like region, *J. Acoust. Soc. Am.* 117 (2005) 1088–1097.
- [20] Y.C. Angel, C. Aristégui, Analysis of sound propagation in a fluid through a screen of scatterers, *J. Acoust. Soc. Am.* 118 (2005) 72–182.
- [21] S. Robert, J.M. Conoir, Reflection and transmission process from a slab-like region containing a random distribution of cylindrical scatterers in an elastic matrix, *Acta Acust. Acust.* 93 (1) (2007) 1–12.
- [22] J.M. Conoir, Essai de synthèse concernant les différents modèles de diffusion multiple qui conduisent au calcul d'un nombre d'onde effectif (Overview on the multiple scattering theories that lead to effective wavenumber calculations), in: *Etude de la propagation ultrasonore en milieux non-homogènes en vue du contrôle non destructif*, journée du GDR-US, Aussois, France, 8–12 décembre 2003, INRIA, Le Chesnay, 2004.
- [23] V. Tournat, V. Pagneux, D. Lafarge, L. Jaouen, Multiple scattering of acoustic waves and porous absorbing media, *Phys. Rev. E* 70 (2004) 026609.1–026609.10.
- [24] A. Derode, V. Mamou, A. Tourin, Influence of correlations between scatterers on the attenuation of the coherent wave in a random medium, *Phys. Rev. E* 74 (2006) 036606.1–036606.9.
- [25] F. Vander Meulen, G. Feuillard, O. Bou Matar, F. Levassort, M. Lethiecq, Theoretical and experimental study of the influence of the particle size distribution on acoustic wave properties of strongly inhomogeneous media, *J. Acoust. Soc. Am.* 110 (2001) 2301–2307.
- [26] R.E. Challis, M.J.W. Povey, M.L. Mather, A.K. Holmes, Ultrasound techniques for characterizing colloidal dispersions, *Rep. Prog. Phys.* 68 (2005) 1541–1637.
- [27] L.M. Brekhovskikh, O.A. Godin, *Acoustics of Layered Media I*, Springer-Verlag, 1990.
- [28] C. Aristégui, Y.C. Angel, Effective mass density and stiffness derived from P-wave multiple scattering, *Wave Motion* 44 (2007) 153–164.
- [29] N.D. Veksler, *Resonance Acoustic Spectroscopy*, Springer-Verlag, 1993.
- [30] A. Ishimaru, *Wave Propagation and Scattering in Random Media*, vol. 2, Academic Press, 1978.
- [31] L.B. Felsen, N. Marcuvitz, *Radiation and Scattering of Waves*, IEEE/OUP Series on Electromagnetic Wave Theory (1994).
- [32] L. Flax, G.C. Gaunard, H. Überall, The theory of resonance scattering, *Physical Acoustics*, vol. XV, Academic Press, New York, 1981, pp. 191–294.